+ MODEL

Genes & Diseases (2024) 11, 100977

Available online at www.sciencedirect.com

ScienceDirect

journal homepage: www.keaipublishing.com/en/journals/genes-diseases

FULL LENGTH ARTICLE

Transcriptomic analysis identifies the neuropeptide cortistatin (CORT) as an inhibitor of temozolomide (TMZ) resistance by suppressing the NF-κB-MGMT signaling axis in human glioma

Zongze He [a,1], Bo Peng [b,1], Qi Wang [a,1], Jie Tian [a,1], Ping Liu [a], Jie Feng [a], Yiwei Liao [c], Longyi Chen [a,***], Ping Jia [a,**], Jian Tang [a,*]

[a] *Department of Neurosurgery, Sichuan Provincial People's Hospital, University of Electronic Science and Technology of China, Chengdu, Sichuan 610072, China*
[b] *Department of Rehabilitation Medicine, Sichuan Provincial People's Hospital, University of Electronic Science and Technology of China, Chengdu, Sichuan 610072, China*
[c] *Department of Neurosurgery, Xiangya Hospital, Central South University, Changsha, Hunan 410008, China*

Received 2 August 2022; received in revised form 19 March 2023; accepted 2 April 2023
Available online 19 June 2023

KEYWORDS
Cortistatin;
Glioma;
MGMT;
NF-κB pathway;
Temozolomide

Abstract Glioma is a common tumor originating in the brain that has a high mortality rate. Temozolomide (TMZ) is the first-line treatment for high-grade gliomas. However, a large proportion of gliomas are resistant to TMZ, posing a great challenge to their treatment. In the study, the specific functions and mechanism(s) by which cortistatin (CORT) regulates TMZ resistance and glioma progression were evaluated. The decreased expression of CORT was detected in glioma tissues, and highly expressed CORT was associated with a better survival rate in patients with glioma. CORT overexpression notably decreased the capacity of glioma cells to proliferate and migrate *in vitro* and to form tumors *in vivo*. CORT overexpression also markedly suppressed the viability and enhanced the apoptosis of TMZ-resistant U251 cells by regulating MGMT, p21, and Puma expression. Importantly, CORT overexpression reduced the resistance of gliomas to TMZ *in vivo*. CORT expression was negatively correlated with MGMT expression in

* Corresponding author.
** Corresponding author.
*** Corresponding author.
E-mail addresses: chenly11@163.com (L. Chen), aonejia@126.com (P. Jia), tangjian@med.uestc.edu.cn (J. Tang).
Peer review under responsibility of Chongqing Medical University.
[1] These authors contributed equally to this work.

https://doi.org/10.1016/j.gendis.2023.04.017

both glioma tissues and cells, and it was found that CORT inhibited NF-κB pathway activation in glioma cells, thereby inhibiting MGMT expression. In conclusion, CORT regulates glioma cell growth, migration, apoptosis, and TMZ resistance by weakening the activity of NF-κB/p65 and thereby regulating MGMT expression. The CORT/NF-κB/MGMT axis might be regarded as a molecular mechanism contributing to the resistance of glioma to TMZ. Our data also suggest that CORT regulates the viability and metastatic potential of glioma cells, independent of its effects on TMZ resistance, providing evidence of novel therapeutic targets for glioma that should be evaluated in further studies.

Introduction

Gliomas are the most common primary brain tumors, accounting for >30% of all primary central nervous system neoplasms.[1,2] The 5-year mortality rate of gliomas is second only to that of pulmonary and pancreatic tumors among systemic tumors.[3] Gliomas cannot be fully cured by conventional treatments such as surgery, radiation, or chemotherapy due to their high aggressiveness and heterogeneity. The median survival time of glioblastoma patients remains 8—12 months.[4,5] As a result, significant efforts are required to better comprehend the pathological process and to uncover innovative therapeutic approaches for this malignant tumor.

Temozolomide (TMZ), a second-generation oral alkylating agent that can easily cross the blood—brain barrier, is now widely applied as a first-line chemotherapy agent for malignant gliomas.[6,7] TMZ causes DNA alkylation damage, primarily at guanine N3, N7, O6, and adenine O3, which induces DNA cross-linking, leading to cancer cell death.[8] Although TMZ has achieved encouraging effects since its clinical application, its effective rate is less than 50% because of the high incidence of drug resistance.[9] TMZ resistance cannot be attributed to a single factor; instead, the possible mechanisms include tumor cells' stress reactions to chemotherapeutic agents, tumor stem cells and their microenvironment, activated DNA damage repair pathways, and the poor permeation of drugs into tumor tissues.[10,11] Among these, MGMT (O6-methylguanine-DNA methyltransferase) is responsible for repairing DNA alkylation damage produced by alkylating drugs such as TMZ.[12,13] Tumor cells with MGMT expression exhibit higher TMZ resistance than those without.[14]

As a major transcription factor involved in inflammation, nuclear factor-κB (NF-κB) is related to gliomas and excessively activated via numerous growth factors and cytokines.[15,16] In a previous report, overactivation of the phosphatidylinositol 3-kinase (PI3K)/AKT/mammalian target of the rapamycin pathway and downstream targets of this pathway, such as NF-κB and p53, was one of the common events observed in glioma.[17] NF-κB mediates the transcription of multiple genes, such as MGMT, to promote resistance to chemotherapy.[18]

Cortistatin (CORT) is a neuropeptide with multiple functions, especially under inflammatory conditions.[19] Although best characterized in inhibitory neurons of the cerebral cortex, CORT is expressed in multiple cells and appears to play a pivotal role in various physiological and disease processes, including immune responses, cardiac diseases, and degeneration of the nervous system.[20—22] CORT is able to bind all five cloned somatostatin receptors and shares many structural, pharmacological, and functional characteristics with somatostatin.[23] CORT has shown protective effects against several cancers, including lung cancer[24] and hepatocellular carcinoma.[25] However, the biological effects of CORT on glioma have not been fully elucidated.

We, therefore, attempted to elucidate the biological functions and underlying molecular mechanism(s) of action of CORT in glioma. High-grade glioma tissues were collected and examined for CORT expression. The effects of CORT on glioma were investigated using viability, migration, apoptosis, and TMZ resistance assays in experiments performed in cells and animals. Moreover, we examined the effects of CORT on the NF-κB-MGMT pathway and whether targeting CORT might represent a potential therapeutic strategy for glioma.

Materials and methods

Clinical tissue samples

A total of 32 glioma tissue samples (10 of grade II, 9 of grade III, and 13 of grade IV) and 6 noncancerous peritumoral brain edema tissue samples (adjacent tissue samples) were obtained from patients undergoing surgical treatment at Sichuan Provincial People's Hospital under the approval of the Ethics Committee of Sichuan Provincial People's Hospital. All enrolled patients provided written informed consent. All tissue samples were kept at −80 °C or fixed in 4% paraformaldehyde before further experiments.

Bioinformatic analysis

The expression data were downloaded in the Gene Expression Omnibus of the National Center of Biotechnology Information (NCBI) with accession numbers GSE147352 and GSE100736. The GSE147352 dataset is the transcriptome profiling of 85 adult glioblastomas, 18 lower-grade gliomas, and 15 normal brain tissues by rRNA-deleted total RNAseq. The analysis for the GSE147352 microarray was based on the GPL20301 platform. Differentially expressed genes were screened using Student's *t*-test ($P < 0.001$) accompanied by the $|\log2 \text{ (fold change)}| > 2$. The GSE100736 dataset is the mRNA expression data from the TMZ-resistant U251 and TMZ-sensitive U251 cell lines.

The CORT expression was analyzed in the TMZ-resistant glioma cell line based on the GSE100736 dataset. Moreover, a survival analysis was applied to determine the link between the expression level of CORT and the prognosis of glioma patients according to the Chinese Glioma Genome Atlas (CGGA, http://www.cgga.org.cn/) and The Cancer Genome Atlas (TCGA)-glioblastoma and low-grade glioma (GBMLGG, https://xenabrowser.net/datapages/).

Hematoxylin and eosin (HE) staining

The histopathological examination of glioma tissues was implemented using HE staining. The glioma tissue samples were fixed for 8 h in 4% formalin solution at 4 °C, put into a 70% ethanol solution for 5 min, and then dehydrated in a gradient of 80%, 90%, 95%, and absolute ethanol, respectively, for 4 h each. Lastly, the glioma tissues were submerged in xylene for 30 min, followed by paraffin embedding. Glioma tissues were then sliced to provide 4-μm-thick coronal sections. After deparaffinization, a light microscope (Olympus, Tokyo, Japan) was employed to observe and photograph the tissues.

Immunohistochemistry (IHC) staining

IHC staining was carried out on glioma tissue sections of 4 μm thickness. Briefly, paraffin-embedded tissue sections were deparaffinized and rehydrated by a graded alcohol series and rinsed 2 times for 10 min per time in phosphate-buffered saline (PBS), followed by incubation with endogenous peroxidase blocking buffer, BSA blocking buffer, and a rabbit polyclonal primary antibody against CORT (Cat# Ab81208, 1/100, Abcam, Cambridge, MA, USA) or ki67 (Cat# Ab16667, 1/200, Abcam) overnight. Next, slices were incubated at 37 °C for 30 min with 45 μL of the secondary antibody, horseradish peroxidase-conjugated goat anti-rabbit IgG H&L (Cat# Ab6721, 1:500, Abcam), then stained for 3 min with 3, 3′-diaminobenzidine solution, and rinsed for 10 min with water. After counterstaining with hematoxylin, slices were rinsed for 10 min with water and then dehydrated and cleaned. At the time, slices were prepared for microscopic examination.

Cell lines, culture, and TMZ treatment

The U251 human glioma cell line (Cat# BNCC337874) was obtained from the BeNa Culture Collection (Beijing, China) and cultured in high glucose Eagle's Minimum Essential Medium (DMEM, Cat# 31331093, GIBCO BRL, Grand Island, USA) supplemented with 10% FBS (Invitrogen, Carlsbad, USA). The cells were cultivated in a 5% CO_2 atmosphere at 37 °C.

TMZ-resistant U251 cells were derived via TMZ dose escalation from the parental U251 cells according to previous studies[26,27] with some modifications. Parental U251 and LN229 cells were gradually exposed to an incremental TMZ concentration from initiation of 0.25 μg/mL, reaching a concentration of 16 μg/mL. U251 cells were exposed to an initial TMZ concentration of 0.25 μg/mL for two weeks. The surviving population of cells was grown to 80% confluence and passaged twice over 15—20 days. The concentration of TMZ was then sequentially increased in the same manner to 1 μg/mL (15 days), 2 μg/mL (15 days), 4 μg/mL (15 days), 8 μg/mL (20 days), and 12 μg/mL (20 days), and finally to the concentration of 16 μg/mL (25 days). The medium was replaced with a medium containing TMZ every 3 or 4 days. The TMZ-resistant cells were then maintained at a dose of 16 μg/mL TMZ for *in vitro* experiments. To avoid acute toxicity caused by the presence of TMZ, TMZ-resistant U251 cells were cultured without TMZ for 1 week before the experiment. The normal U251 cells were regarded as TMZ-sensitive U251 cells.

Cell transfection

Plasmids constructed with CORT fragments (CORT oe; GenePharma, Shanghai, China) and were transfected into U251 cells to achieve the overexpression of CORT. Plasmids constructed with short hairpin RNA targeting CORT (sh-CORT1 and sh-CORT2) were used to achieve the knockdown of CORT. The sequences of overexpressing vector and shRNA vector are listed in Table 1. The Lipofectamine® 3000 reagent (Invitrogen) was utilized for all transfections. Cells were transfected for 48 h and collected for subsequent studies.

PCR (polymerase chain reaction)-based analysis

To determine the RNA expression levels, total RNA was isolated from target cells or tissues using the Trizol reagent (Invitrogen) as directed by the manufacturer's protocol. A First-strand cDNA Synthesis Kit (Promega, Madison, WI, USA) was utilized to reverse-transcribe the RNA. Next, the QuantiTect SYBR Green PCR Kit (Qiagen, Germantown, MD, USA) was employed to examine the expression levels according to the manufacturer's protocol. The $2^{-\Delta\Delta Ct}$ method was utilized to calculate the relative expression values by using the GAPDH expression as an internal control. The primer sequences used in the PCR assay are listed in Table 1.

Immunoblotting

The total protein was isolated from cells and tissues using RIPA lysis buffer (Thermo Fisher Scientific, Waltham, USA). After quantitative analysis using the bicinchoninic acid method, 50 μg of total protein were separated by SDS-PAGE (polyacrylamide gel electrophoresis), and transported onto PVDF (polyvinylidene difluoride) membranes. Membranes were blocked for 1 h with TBS-T buffer supplemented with 5% non-fat milk and then incubated at 4 °C overnight with primary antibodies such as anti-CORT (Cat# ab81208, 1/50000, Abcam), anti-PCNA (Cat# ab29, 1/1000, Abcam), anti- MMP2 (Cat# ab92536, 1/1000, Abcam), anti-MMP9 (Cat# ab76003, 1/1000, Abcam), anti-MGMT (Cat# ab39253, 1/1000, Abcam), anti-p21 (Cat# ab109520, 1/1000, Abcam), anti-Puma (Cat# ab9643, 1/2000, Abcam), anti-Cleaved-caspase 3 (Cat# ab32042, 1/500, Abcam), anti-caspase 3 (Cat# ab32351, 1/5000, Abcam), anti-p50 (Cat# ab32360, 1/1000, Abcam), anti-p65 (Cat# ab32536, 1/1000, Abcam), GAPDH (T0004, 1/3000, Affinity, USA), Histone H3 (Cat# Ab1791, 1/1000, Abcam), and β-Tubulin (Cat# ab6046, 1/1000, Abcam). Membranes were washed with TBS three times, followed by incubation at 25 °C for 1.5 h with an HRP (horseradish peroxidase)-conjugated secondary antibody, goat anti-rabbit IgG H&L or goat anti-mouse IgG H&L (Cat# ab97051 and

Table 1 The primer sequence for the study.

	Gene	Primer	Sequence (5′-3′)
PCR primer	CORT	Forward	GCCTCCTGACTTTCCTCGC
		Reverse	GGGCTTCCTCTCCTATGAGGG
	MGMT	Forward	TTTTCCAGCAAGAGTCGTTCAC
		Reverse	GGGACAGGATTGCCTCTCAT
	CIDEA	Forward	GATGCCCTCGTCATCGCTAC
		Reverse	GCGTGTTGTCTCCCAAGGTC
	FAM163A	Forward	GCTCCCACATACTACAAAGAGGG
		Reverse	CCAGGTCACCGGGTAACTC
	KLK5	Forward	TCTCGGCCACTACTCCCTG
		Reverse	AGACGTTGATGGGTCTGACAT
	CALHM1	Forward	GCTGGCCGAAGAGTGGAAG
		Reverse	CATTTGCCGTCGAGTAGCG
	ANKRD34C	Forward	TGTGCGTCTCCCTCTGACATA
		Reverse	GGAGGTGTTACAACTGCTTGGA
	CTXN3	Forward	GCCCCTTGGGAACGAATCAG
		Reverse	AGCACCGGACAATGAGAATGC
	ABCG8	Forward	AGGCCCAGCGTGACAAAAG
		Reverse	TGGGTTCGTCGAGAATAAGGA
	CREB3L3	Forward	GCCCTGCCTCTCCTATCATC
		Reverse	ACGGTGAGATTGCATCGTGG
	MYADML2	Forward	GTCTTCTGTTTCGATCCCAAGT
		Reverse	GAGGTCAACGACGTACAGGAG
	GAPDH	Forward	ACAGCCTCAAGATCATCAGC
		Reverse	GGTCATGAGTCCTTCCACGAT
Vector primers	Vector NC	Forward	/
		Reverse	/
	CORT OE	Forward	CTAGCGTTTAAACTTAAGCTTATGCCATTGTCCCCCGGC
	(pcDNA3.1)	Reverse	TGCTGGATATCTGCAGAATTCTTATTTGCAGGAGGAGAAGGTCTT
	sh-NC	Forward	GATCCGCAGATGAAGGCACGGTCACGCTCGAGGCAGATGAAGGCACGGTCACGTTTTTG
		Reverse	AATTCAAAAAGCAGATGAAGGCACGGTCACGCTCGAGGCAGATGAAGGCACGGTCACG
	sh-CORT #1	Forward	GATCCGTTTGTTATTTAAATTCCAATCTCGAGATTGGAATTTAAATAACAAACTTTTTG
		Reverse	AATTCAAAAAGTTTGTTATTTAAATTCCAATCTCGAGATTGGAATTTAAATAACAAACG
	sh-CORT #2	Forward	GATCCGATATGAATTGTCTAATTTAACTCGAGTTAAATTAGACAATTCATATCTTTTTG
		Reverse	AATTCAAAAAGATATGAATTGTCTAATTTAACTCGAGTTAAATTAGACAATTCATATCG

ab6789, 1:5000, Abcam). An ECL system (Life Technologies Corporation, Gaithersburg, MD, USA) was employed to carry out signal detection. GAPDH, Histone H3, or β-Tubulin was used as an endogenous total protein, nuclear protein, or cytoplasm protein control, respectively.

Cell counting kit-8 (CCK-8)

Cell proliferation was detected using CCK-8 reagents (Tsbiochem, Shanghai, China). Briefly, cells were plated at a density of 2×10^3 cells/well onto a 96-well plate, followed by incubation for 0 h, 24 h, 48 h, or 72 h. At the indicated time points, 10 μL of CCK-8 was added, followed by another incubation for 4 h. The absorbance at 450 nm was measured using a SpectraMax M5 microplate reader (Molecular Devices, Sunnyvale, CA, USA).

EdU assay

The Click-IT EdU Alexa Fluor 594 kit detects the incorporation of the thymidine analogue 5-ethoxy-2-deoxyuridine (EdU) into genomic DNA during DNA synthesis. Cells that had been treated or transfected were incubated in media supplemented with 10 μmol/L EdU, and the medium was replaced with an EdU-free medium 2 h later. Cells were then fixed and stained with Click-iT solution for 30 min and 4′,6-diamidino-2-phenylindole (DAPI) for 3 min, and a fluorescence microscope was utilized to examine EdU-positive cells. The EdU incorporation rate was determined as the ratio of EdU-positive cells (red cells) to DAPI-positive cells (blue cells).

Transwell assay

Transfected or control cells were brought into suspension by exposure to trypsin and collected for cell counting. Cells were loaded into the upper chamber at a density of 5×10^3 cells in 200 μL serum-free medium, and the lower chamber was filled with 500 μL DMEM with 10% FBS. Following 24 h of culture, cells failing to migrate were removed. The membrane was then rinsed with PBS twice, fixed in 4% methanol solution for 20 min, and stained with 0.1% crystal violet for 30 min. After the membranes were

washed twice in PBS, migrated cells were photographed under a microscope. The observed cell number was evaluated to detect cell migration.

Detection of apoptosis

To detect cell apoptosis, cell digestion was performed with trypsin solution without EDTA, and target cells were resuspended in 500 μL of binding buffer. Next, 5 μL of Annexin V-FITC (Invitrogen, Carlsbad, CA, USA) and 5 μL of propidium iodide (PI; Invitrogen) were added, followed by incubation for 15 min in the dark at ambient temperature. Cell apoptosis was assessed using flow cytometry after the incubation (BD, Franklin Lakes, NJ, USA).

Nude mouse tumorigenicity assay

U251 cells transfected with lv-NC, lv-CORT, lv-sh-NC, lv-sh-CORT1, and lv-sh-CORT2 were harvested during the logarithmic growth phase and resuspended in serum-free medium at 1×10^7 per milliliter. Then, a 0.2-mL aliquot of the cell suspension was subcutaneously injected into the left axillary area of 4-week-old BALB/c nude mice (weighing 18—20 g, purchased from the Laboratory Animal Research Institute of Sichuan Provincial People's Hospital). When all groups showed tumor formation (approximately one week after injection), mice were injected intraperitoneally with TMZ or DMSO (30 mg/kg/day) every 3 days for another 3 weeks.[28] At 28 days, the length (mm), width (mm), and height (mm) of tumor tissues were measured using a vernier caliper; the tumor volume was estimated using the following formula: volume = length × width^2/2. All mice were sacrificed 28 days post-tumor implantation, and the tumor tissues were harvested for the subsequent analyses.

Nuclear and cytoplasmic protein isolation

The nuclear and cytoplasmic proteins were isolated using a nuclear/cytosol fractionation kit (P0027, Beyotime, China). U251 cells were rinsed twice and harvested in ice-cold PBS for cell counting. Following centrifugation for 5 min at 2000 *g*, the sediment was dissolved by vortexing for 5 s in 1 mL protein extraction reagent B and then was incubated for 1 min on ice. After clearing the lysates by centrifugation (14,000 *g*, 10 min), the cytoplasmic protein was obtained by collecting the supernatant. The precipitates were further lysed in a nuclear protein isolation reagent for 30 min. Following centrifugation (14,000 *g*, 10 min), the supernatant protein was harvested as the pool of nuclear proteins. A Pierce BCA protein assay was then applied to determine the protein concentration (μg/million cells). Subsequently, a histone H3 antibody and β-tubulin antibody were utilized as endogenous controls to confirm the separation of nuclear and cytoplasmic proteins, respectively.

Immunofluorescent (IF) staining

The p65 levels were detected using primary antibodies against p65 (Cat# ab32536, 1/100, Abcam), and a FITC-labeled goat anti-rabbit IgG was used as the secondary antibody in IF staining. Briefly, target cells were grown on coverslips and then plated in DMEM with FCS, followed by incubation for 24 h to achieve effective attachment. Then, the cells were washed with PBS, fixed in 4% paraformaldehyde, permeabilized in triton-100, and blocked in PBS buffer containing 5% bovine serum albumin. In the blocking buffer, the coverslip was incubated with the aforementioned primary antibody and FITC-labeled goat anti-secondary antibody (1:400) against rabbit IgG. Finally, the fluorescent signals were examined using a fluorescent microscope (Olympus, Japan).

Statistical analysis

The animal experiments were conducted at least 6 independent times. The cell experiments were conducted at least 3 independent times. The data were expressed as mean ± standard deviation (SD). The SPSS20.0 statistical software was employed to carry out statistical calculations. The differences between two experimental groups were compared using Student's *t*-test. Assessments of three or more groups were performed using a one-way ANOVA. A *P*-value ≥0.05 means that no effect was observed.

Results

Decreased CORT expression is associated with unfavorable clinical outcomes for glioma patients

Human glioma and normal brain tissue specimens were examined for differentially expressed genes (DEGs) using the GSE147352 dataset, and 2024 DEGs were obtained. Then, 33 DEGs related to glioma patients' overall survival (OS) were found based on CGGA and TCGA-GBMLGG datasets. Among them, 11 DEGs were protective factors for glioma patients; 10 of the DEGs (*CIDEA*, *FAM163A*, *KLK5*, *CALHM1*, *ANKRD34C*, *CTXN3*, *ABCG8*, *CREB3L3*, *MYADML2*, and *CORT*) were down-regulated in glioma tissues according to GSE147352 dataset (Fig. S1A). Next, a real-time PCR assay was performed to determine the mRNA expression of the above 10 DEGs in glioma and normal tissues (Fig. S1B). Among them, the expression of CORT was the lowest in glioma tissues. CORT is a neuropeptide that is abundant in the brain[29] and has been reported to be associated with neural activity[30,31] and cancer pathogenesis.[21] Therefore, CORT was chosen as the target for additional studies. Further verification showed that CORT expression was dramatically decreased in glioma tissue samples in the GSE147352 dataset (Fig. 1A). The expression of CORT in the CGGA and TCGA-GBMLGG datasets was related to the glioma patients' OS; high expression of CORT could predict considerably better overall survival among the glioma patients (Fig. 1B, C). To validate the CORT expression within glioma tissues, clinical noncancerous peritumoral brain edema (adjacent) tissue samples and high-grade glioma (grade II, III, and grade IV) samples were collected and examined. As shown by HE staining, noncancerous samples showed no definitive neoplastic cells, with a high degree of cytoarchitectural preservation, such as clearly differentiated neurons. Tissue samples of grade II, III, and grade IV glioma showed abundant tumor cellularity with high infiltration of tumor cells and no preserved adjacent normal

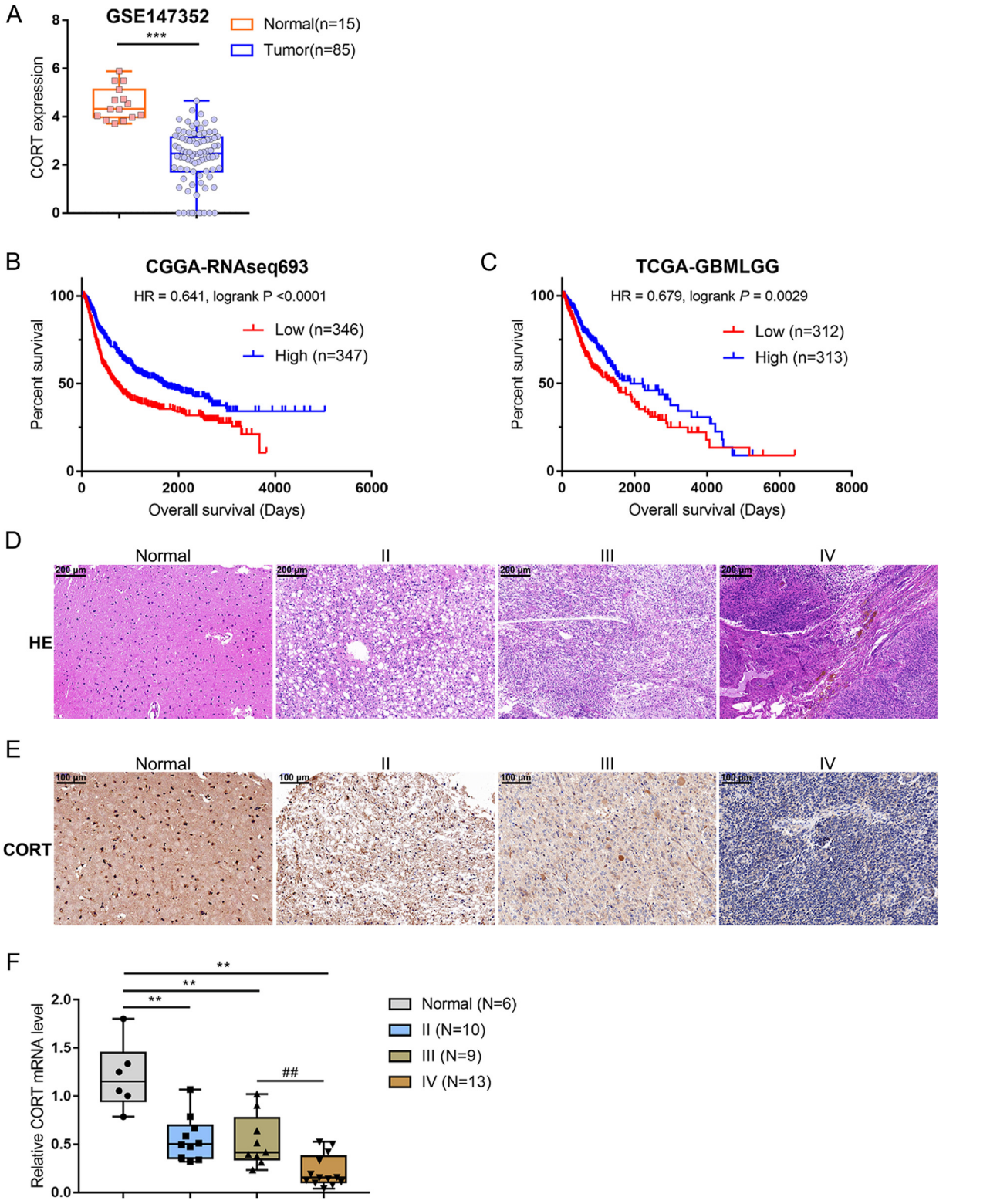

Figure 1 Expression of CORT in glioma tissue samples. **(A)** The differences in the expression of CORT in glioma tissue samples based on the GSE147352 dataset. **(B, C)** Correlation between the overall survival (OS) and CORT expression in patients with glioma based on the CGGA and TCGA-GBMLGG datasets. **(D)** Clinical samples of noncancerous peritumoral brain edema (adjacent) tissue and different grades of glioma were collected and examined for histopathological characteristics by HE staining. Scale bar = 200 μm. **(E)** The protein content and distribution of CORT in noncancerous adjacent normal cases and high-grade glioma tissue samples (grade II, III, and grade IV) were determined by IHC staining. Scale bar = 100 μm. **(F)** The mRNA expression levels of CORT were determined in noncancerous adjacent normal samples ($n = 6$) and glioma tissue samples ($n = 10$ for grade II glioma, $n = 9$ for grade III glioma, and $n = 13$ for grade IV glioma) by real-time PCR.

brain cytoarchitecture (Fig. 1D). IHC staining showed that CORT expression was reduced in high-grade glioma tissues (Fig. 1E). The real-time PCR results similarly showed that the mRNA expression of CORT was dramatically lower in grade II, III, and IV glioma tissue samples (Fig. 1F). These results show that there is decreased expression of CORT in glioma tissues, which suggests that it might be associated with a worse survival rate of patients with glioma.

CORT inhibits the proliferation and migration of glioma cells

To assess the specific roles of CORT in different glioma cell phenotypes, CORT was overexpressed in U251 cells by transfecting them with a CORT overexpression vector (CORT oe). The overexpression was confirmed by Western blotting (Fig. 2A). As shown by the CCK-8 and EdU assays, U251 cell proliferation was dramatically repressed by CORT overexpression (Fig. 2B, C). CORT overexpression also notably decreased U251 cell migration (Fig. 2D). Next, two plasmids inserted with shRNA specifically targeting CORT (sh-CORT) were constructed and transfected into U251 cells, and reduced CORT protein expression was confirmed by Western blotting (Fig. 2E). The U251 cells with reduced CORT expression had increased viability (Fig. 2F), proliferation (Fig. 2G), and migration (Fig. 2H) compared to the control cells. These results all suggest that CORT exerts anti-cancer effects in glioma cells.

CORT alleviates glioma tumor growth in nude mice *in vivo*

A mouse tumor xenograft model was constructed to investigate the roles of CORT in glioma *in vivo*. First, we pretransfected U251 cells with plasmids to induce CORT overexpression or silencing; next, these cells were subcutaneously injected into the dorsal area of nude mice. The experiment was terminated by the sacrifice of surviving mice and excision of tumors on day 25 (Fig. 3A). The increases in tumor weight (Fig. 3B) and tumor volume (Fig. 3C) were dramatically repressed by CORT overexpression and notably increased CORT silencing. The IHC staining indicated that CORT overexpression inhibited Ki-67 protein expression and promoted CORT protein expression. In contrast, CORT silencing showed the opposite trends (Fig. 3D). CORT overexpression also reduced the expression levels of the PCNA, MMP2, and MMP9 proteins, which are related to cell proliferation and migration. In contrast, CORT knockdown increased the PCNA, MMP2, and MMP9 protein expression levels (Fig. 3E). In summary, CORT overexpression significantly reduced the growth and progression of glioma *in vivo*.

CORT is negatively correlated with MGMT in glioma tissues and cells

The mRNA expression of MGMT was notably higher in grade II and III glioma tissue samples and the highest within grade IV glioma tissue samples (Fig. 4A). Moreover, the CORT expression was negatively correlated with the MGMT expression in glioma tissues ($r = -0.6772$, $P < 0.0001$, Fig. 4B). TMZ resistance in glioma remains a huge challenge to treatment. Therefore, the expression of CORT within TMZ-resistant glioma cells was detected to investigate its potential involvement in the resistance of glioma to TMZ. It was observed that CORT was dramatically down-regulated within the TMZ-resistant glioma cell line according to the GSE100736 dataset (Fig. 4C). As previously reported, MGMT is linked to the resistance of glioma to TMZ.[13,32] MGMT was notably up-regulated within the TMZ-resistant glioma cell line in the GSE100736 dataset (Fig. 4D). CORT expression exhibited a markedly negative correlation with MGMT expression in the TMZ-resistant glioma cell in this dataset ($r = -0.9536$, $P = 0.0032$, Fig. 4E). Next, TMZ-sensitive and -resistant U251 cells were established and treated with 0.25, 1, 4, 16, or 64 μg/mL TMZ. The cell viability was determined and shown as IC50 values. As indicated in Figure 4F, the IC50 values for TMZ-resistant U251 cells were elevated compared with TMZ-sensitive U251 cells. Compared to TMZ-sensitive U251 cells, the CORT protein expression was suppressed, while the MGMT protein level was elevated in the TMZ-resistant U251 cells (Fig. 4G).

CORT recedes glioma cell resistance to TMZ

To further investigate the effects of CORT on the resistance of glioma to TMZ, CORT was overexpressed or knocked down in TMZ-resistant U251 cells for 48 h. Next, Western blotting was conducted to detect the expression of the MGMT, p21, and Puma proteins (Fig. 5A). CORT overexpression inhibited MGMT protein expression while promoting the expression of the p21 and Puma proteins. In contrast, the knockdown of CORT led to the opposite effects. Then, the transfected resistant U251 cells were treated with TMZ (16 μg/mL) and examined for cell viability and apoptosis. CORT overexpression dramatically suppressed cell viability (Fig. 5B) and enhanced cell apoptosis (Fig. 5C). In contrast, CORT silencing notably enhanced cell viability (Fig. 5B) and suppressed cell apoptosis (Fig. 5C). These experiments suggested that CORT reduces the resistance of glioma cells to TMZ.

CORT weakens glioma resistance to TMZ *in vivo*

To confirm the effects of CORT on the TMZ resistance of glioma cells *in vivo*, a subcutaneous xenograft tumor model of TMZ-resistant U251 cells was established in nude mice. Both CORT overexpression and TMZ treatment significantly decreased the tumor weight and volume when used alone. However, the combination of CORT overexpression with TMZ led to increased anti-tumor effects compared to either treatment alone (Fig. 6A–C). To elucidate the molecular mechanism(s) responsible for these findings, we examined the protein levels of factors associated with drug resistance and apoptosis (MGMT, p21, Puma, and cleaved-caspase 3/caspase 3). Either CORT overexpression or TMZ treatment notably inhibited the MGMT protein expression and increased the expression levels of p21, Puma, and cleaved-caspase 3/caspase 3. The effects of TMZ on these markers were enhanced by CORT overexpression (Fig. 6D). Thus, these results confirmed that CORT reduces the resistance of glioma to TMZ *in vivo*.

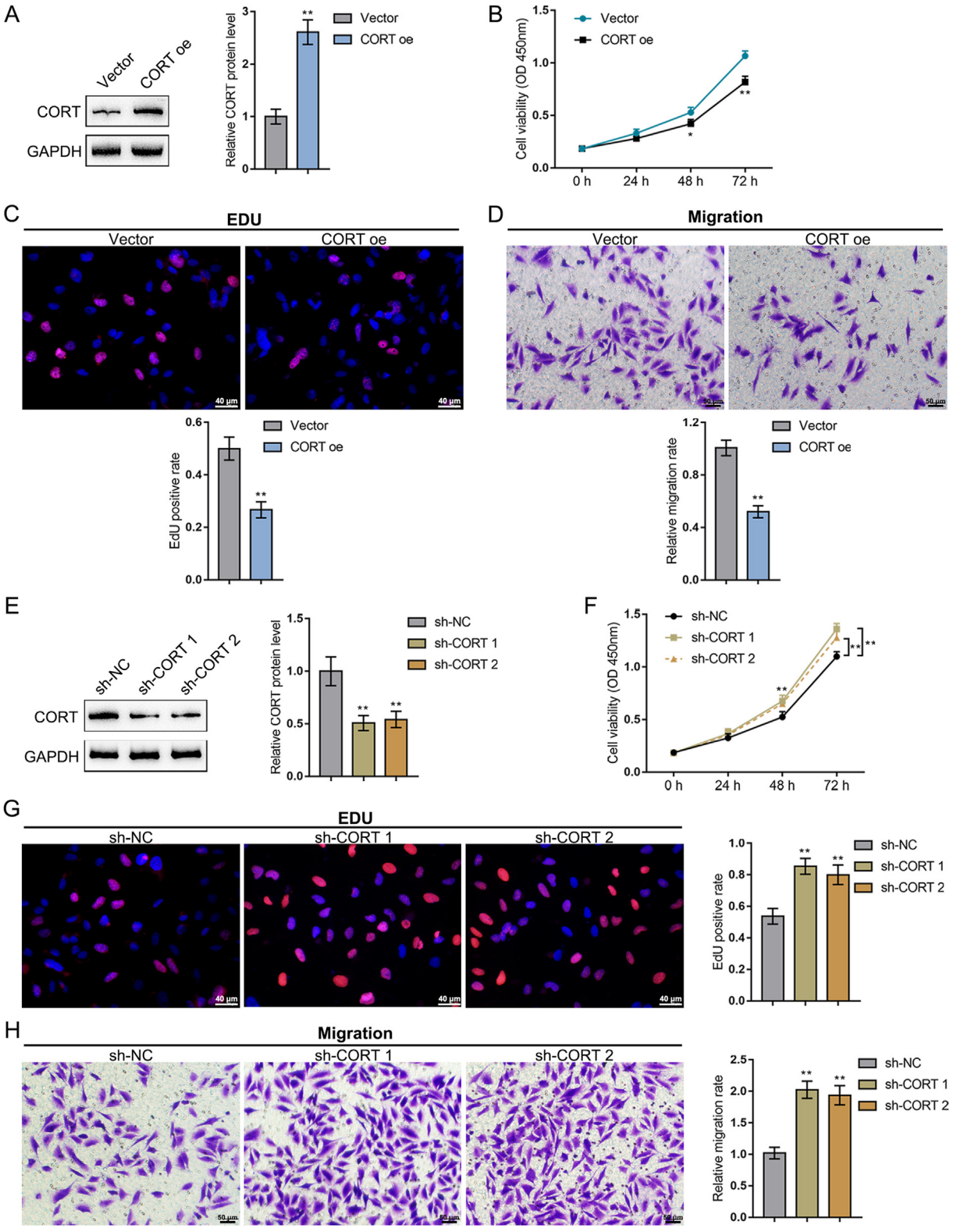

Figure 2 Effects of CORT on the proliferation and migration of glioma cells. **(A)** CORT was overexpressed in U251 cells by transfecting them with a CORT overexpression vector (CORT oe), and the successful transfection was confirmed by Western blotting. **(B—D)** U251 cells were transfected with CORT oe and examined for cell viability by the CCK-8 assay (B), DNA synthesis by the EdU assay (C), and cell migration by the Transwell assay (D). **(E)** Two plasmids inserted with shRNA specifically targeting CORT (sh-CORT) were constructed and transfected into U251 cells, and the impact on CORT expression was confirmed by Western blotting. **(F—H)** U251 cells were transfected with the CORT knockdown plasmid and examined for cell viability by the CCK-8 assay (F), DNA synthesis by the EdU assay (G), and cell migration by the Transwell assay (H). Scale bar = 40 or 50 μm. $n = 3$; $^{*}P < 0.05$, $^{**}P < 0.01$, compared with the vector or sh-NC group.

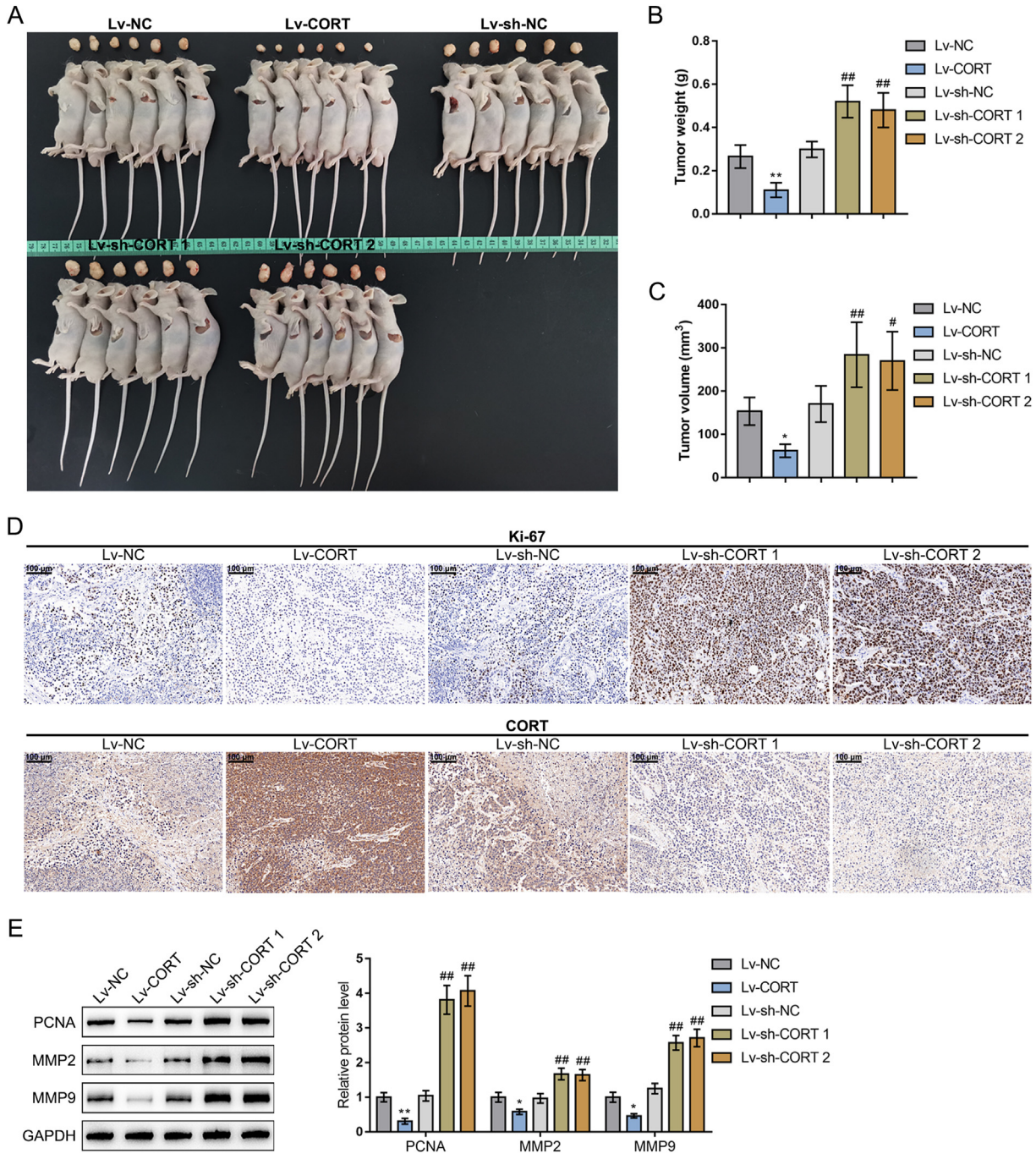

Figure 3 Effects of CORT on the growth of glioma *in vivo*. **(A)** A subcutaneous xenotransplant tumor model was established in nude mice by injecting U251 cells transfected with the CORT overexpression or silencing plasmid. At the termination of the experiment (on the 25th day after tumor cell injection), we sacrificed the mice and excised the tumors. The images of the tumors are shown. **(B, C)** When the nude mice were sacrificed on the 25th day, the tumor weight (B) and volume (C) were measured. **(D)** The protein expression levels of Ki-67 and CORT in glioma tissue samples were detected by IHC staining. **(E)** The levels of proteins associated with proliferation and migration (PCNA, MMP2, and MMP9) were detected by Western blotting. Scale bar = 100 μm. $n = 6$; $^{*}P < 0.05$, $^{**}P < 0.01$, compared with the lv-NC group; $^{\#}P < 0.05$, $^{\#\#}P < 0.01$, compared with the lv-sh-NC group.

CORT inhibits the activation of the NF-κB pathway

Inhibition of the NF-kB pathway has previously been shown to down-regulate MGMT expression, thereby improving the chemotherapeutic effects of TZM on glioma.[18,33] Therefore, we hypothesized that CORT inhibited NF-κB pathway activation in glioma, thereby inhibiting MGMT expression and reducing the resistance of glioma to TMZ. Western blotting was performed to detect the effects of CORT on the p50 and p65 (NF-κB subunit) protein contents

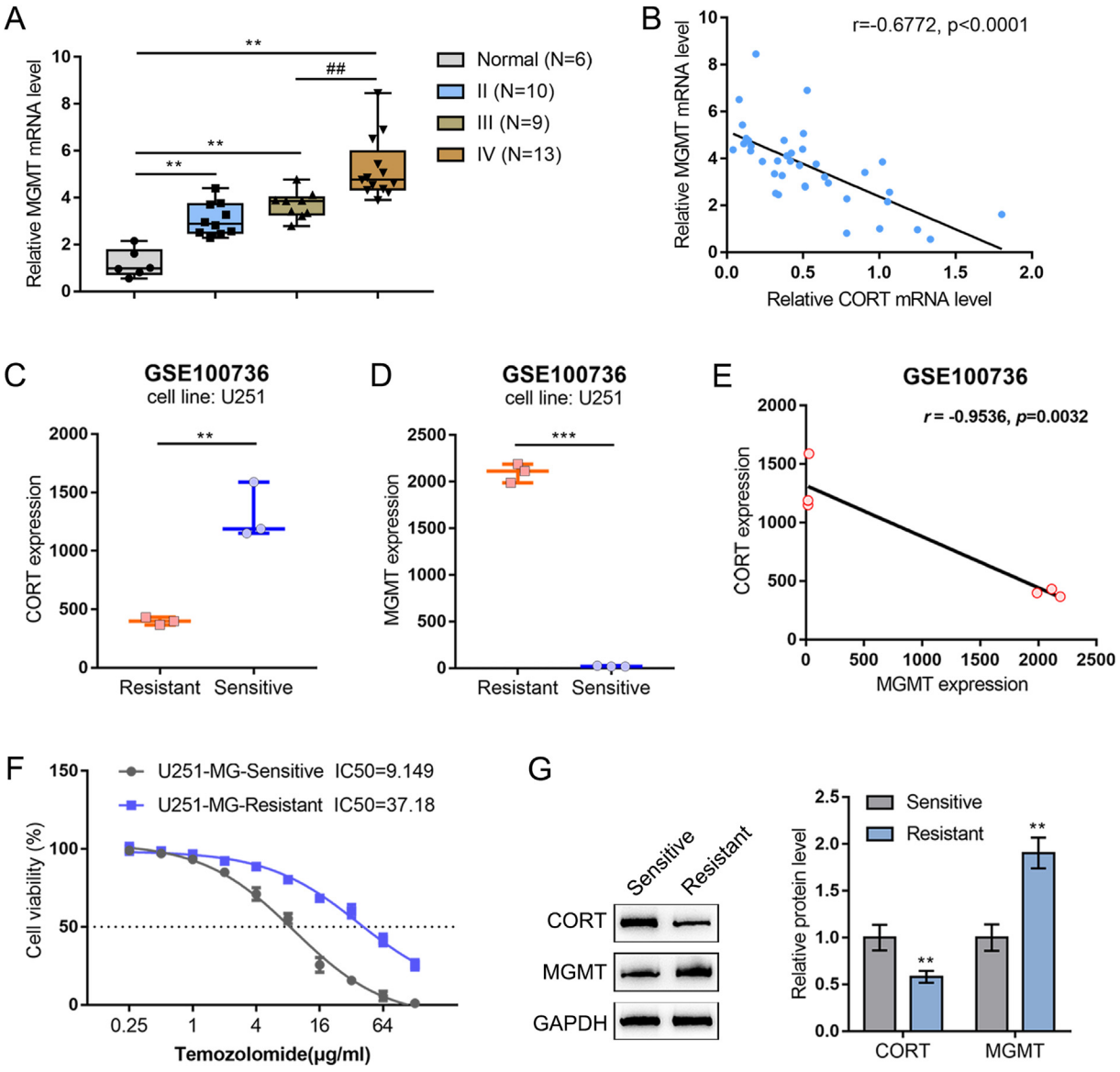

Figure 4 The CORT and MGMT expression levels in TMZ-resistant glioma cells. **(A)** The mRNA expression levels of MGMT were determined in noncancerous adjacent normal tissue samples ($n = 6$) and glioma tissue samples ($n = 10$ for tissue samples of grade II glioma, $n = 9$ for grade III glioma, and $n = 13$ for grade IV glioma) by real-time PCR. **(B)** A linear analysis confirmed the negative correlation between CORT and MGMT expression in glioma. **(C)** The CORT expression in TMZ-resistant glioma cells (U251) according to the GSE100736 dataset. **(D)** The MGMT expression in TMZ-resistant glioma cells (U251) according to the GSE100736 dataset. **(E)** A negative correlation between CORT and MGMT was verified in TMZ-resistant glioma cells based on the GSE100736 database. **(F)** TMZ-sensitive and -resistant U251 cells were exposed to 0.25, 1, 4, 16, or 64 μg/mL TMZ and examined for cell viability by the CCK-8 assay. The IC50 values were calculated and are shown. **(G)** The protein levels of CORT and MGMT in TMZ-sensitive and -resistant U251 cells were detected by Western blotting. $n = 3$; $^{**}P < 0.01$, $^{**}P < 0.001$, compared with TMZ-sensitive U251 cells.

within U251 cells (Fig. 7A). CORT overexpression markedly decreased the expression of both subunits, whereas CORT inhibition elevated the protein expression of both subunits. In agreement with this finding, IF staining showed that the p65 protein level was decreased by CORT overexpression, whereas it was increased by CORT silencing (Fig. 7B). CORT overexpression significantly boosted the phosphorylation of p65 in the nucleus, while CORT silencing inhibited the phosphorylation of p65 in the nucleus. There were no significant effects of CORT on the p65 expression in the cytoplasm (Fig. 7C). Several studies have reported that p65 promotes the transcription of MGMT.[34–36] These data suggest that CORT inhibits the activation of the NF-κB pathway in glioma cells, thereby inhibiting MGMT expression.

Discussion

Glioma is the most prevalent primary brain tumor. The limitations associated with existing therapeutic options make malignant gliomas difficult to treat.[37] CORT, a natural SRIF-like peptide, inhibits neoplastic development in

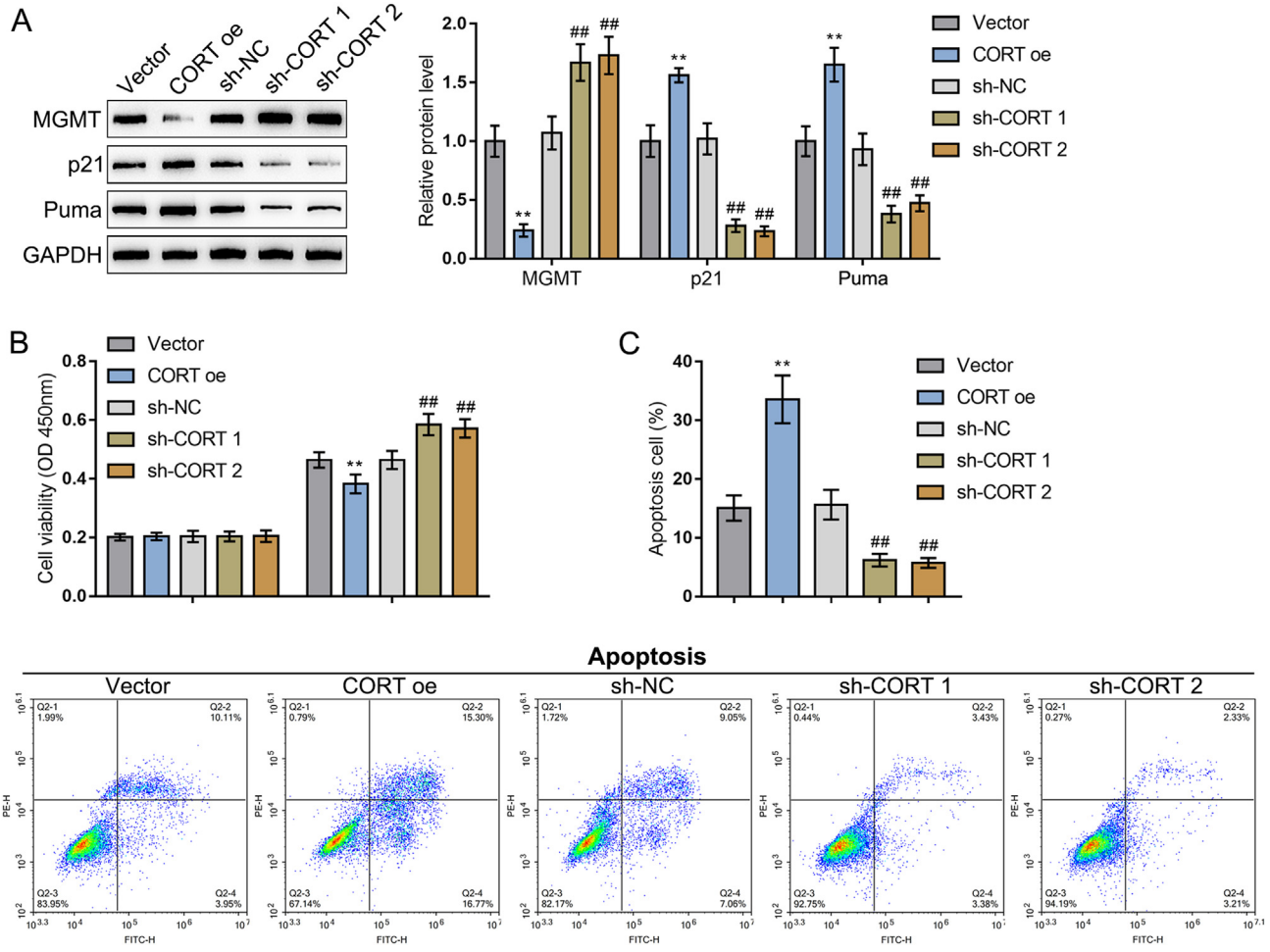

Figure 5 The effects of CORT on the resistance of glioma cells to TMZ. **(A)** TMZ-resistant U251 cells were transfected with a CORT overexpression or knockdown vector, and then the protein expression levels of MGMT, p21, and Puma were detected by Western blotting. **(B, C)** TMZ-resistant U251 cells were transfected with a CORT overexpression or knockdown vector and then exposed to 16 μg/mL TMZ. Cell viability was determined by the CCK-8 assay (B), and cell apoptosis was determined by flow cytometry (C). $n = 3$; $^{**}P < 0.01$, compared with the vector group control; $^{\#\#}P < 0.01$, compared with the sh-NC group.

various malignancies.[38] Cassoni et al elucidated that CORT reduces the proliferation of follicular cell-derived and parafollicular cell-originated human thyroid carcinoma cells.[39] Luque et al proposed that endogenous CORT impacts 7,12-dimethyl-benza-anthracene (DMBA)-induced mammary gland tumorigenesis.[40] However, to our best knowledge, the functions of CORT in glioma were largely unknown. Here, we first revealed that there is decreased expression of CORT in glioma tissues, which might be associated with a worse survival rate of patients with glioma. Then, the specific roles of CORT on glioma cell phenotypes indicated that CORT overexpression notably decreased the capacity of glioma cells to proliferate and migrate *in vitro* and form tumors *in vivo*. The present findings indicate that CORT is strongly associated with glioma development and/or progression.

TMZ is a traditional chemotherapy agent used as an adjuvant treatment for individuals with high-risk gliomas, ranging from grade II to IV.[41] Nevertheless, resistance to TMZ reduces the efficacy of glioma treatment, and glioma patients' survival time remains rather short, averaging approximately one year following TMZ treatment.[42] The present study demonstrated that CORT appears to play a role in the resistance of glioma to TMZ, and suggested the potential mechanism responsible for these effects. We observed that CORT was significantly down-regulated in glioma cells with resistance to TMZ. CORT overexpression dramatically suppressed the viability and enhanced the apoptosis of TMZ-resistant U251 cells by regulating MGMT, p21, and Puma expression. Furthermore, the subcutaneous tumor model in nude mice confirmed that CORT overexpression also reduces TMZ resistance in glioma *in vivo*.

The DNA-repair enzyme MGMT repairs TMZ-induced DNA guanine lesions by transferring the alkyl group from the O^6 site to its cysteine residues.[12,43] It has previously been reported that MGMT is critical for TMZ resistance in glioma.[13,32] Activated NF-κB is a crucial glioma-related transcription factor involved in multiple aspects of cancer progression, including the suppression of invasion, apoptosis, inflammation, and the immune response.[44,45] The activation of NF-κB is initiated in response to treatment with cytotoxic drugs, and TMZ activates NF-κB by

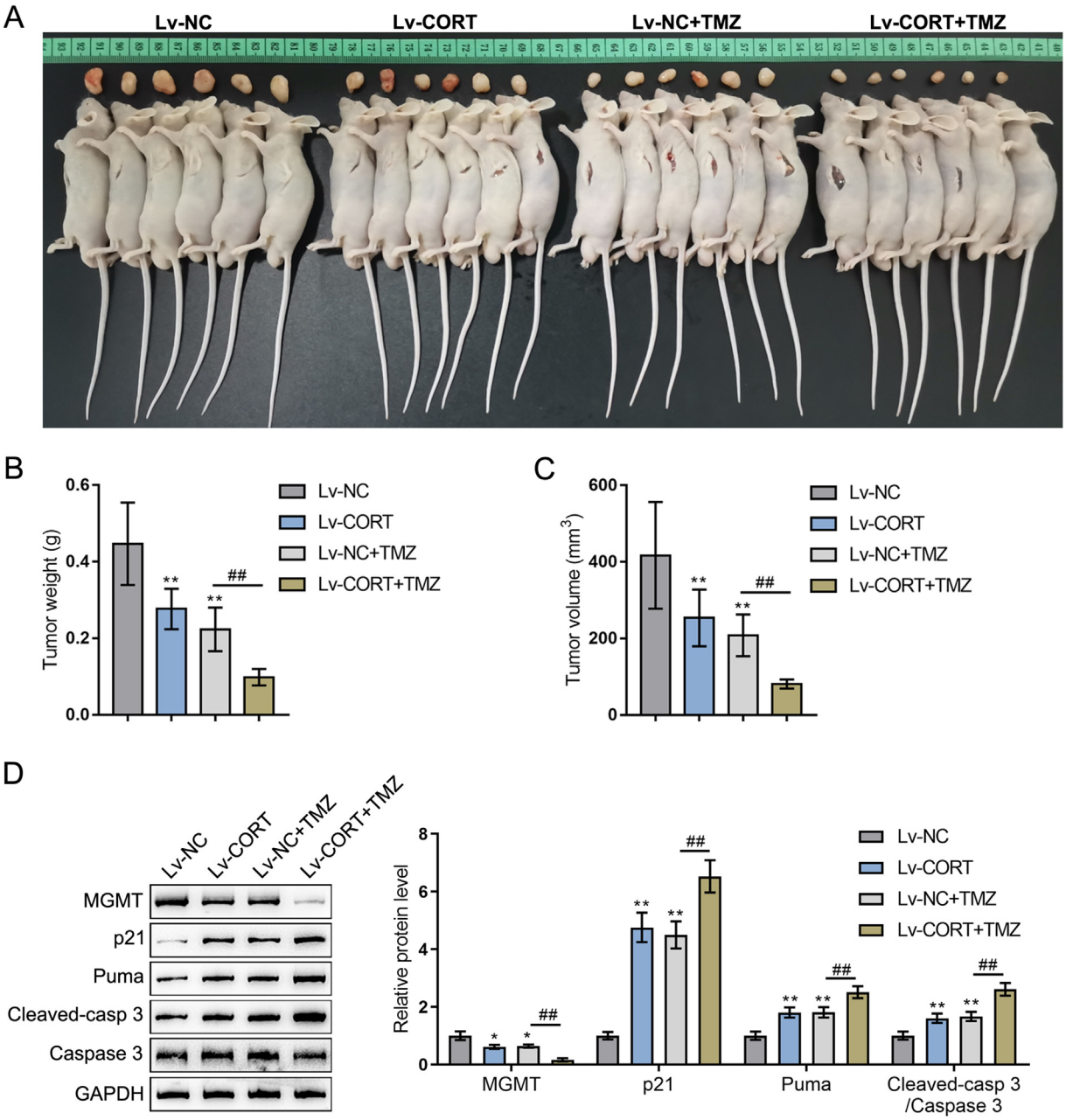

Figure 6 *In vivo* effects of CORT on the TMZ resistance of glioma. **(A)** A subcutaneous tumor model was established in nude mice as described in the Methods. Tumor-bearing mice received TMZ treatment or CORT overexpression, and the tumor images are shown. **(B, C)** The tumor weight and volume were examined upon the excision of tumors on day 25 after injection. **(D)** The protein levels of drug resistance- and apoptosis-related factors (MGMT, p21, Puma, and cleaved-caspase 3/caspase 3) were determined by Western blotting. $n = 6$; $^{*}P < 0.05$, $^{**}P < 0.01$, compared with the lv-NC group; $^{\#\#}P < 0.01$, compared with the lv-NC + TMZ group.

activating the DNA damage pathway.[46,47] Moreover, several studies have reported that the p65 subunit of NF-κB, a transcriptional regulator of MGMT, promotes MGMT expression.[36,48] In this study, CORT overexpression markedly decreased the p50 and p65 protein expression, while CORT inhibition had the opposite effect. CORT reduced the NF-κB/p65-mediated regulation of MGMT expression by disrupting NF-κB signaling in glioma cells, and the CORT/NF-κB/MGMT axis might be regarded as a potential molecular regulator of the resistance of glioma to TMZ.

Nevertheless, there are some limitations associated with this study that need to be considered. First, it has been suggested that several molecular mechanisms are involved in the TMZ resistance of glioma. CORT may also regulate one or more of these other pathways. Second, since all our experiments were conducted on cells and mice, these findings may not be generalizable to humans. In future studies, we may employ experiments in other tumor animal models, such as rabbits or rats, in addition to performing additional studies on patient-derived samples.

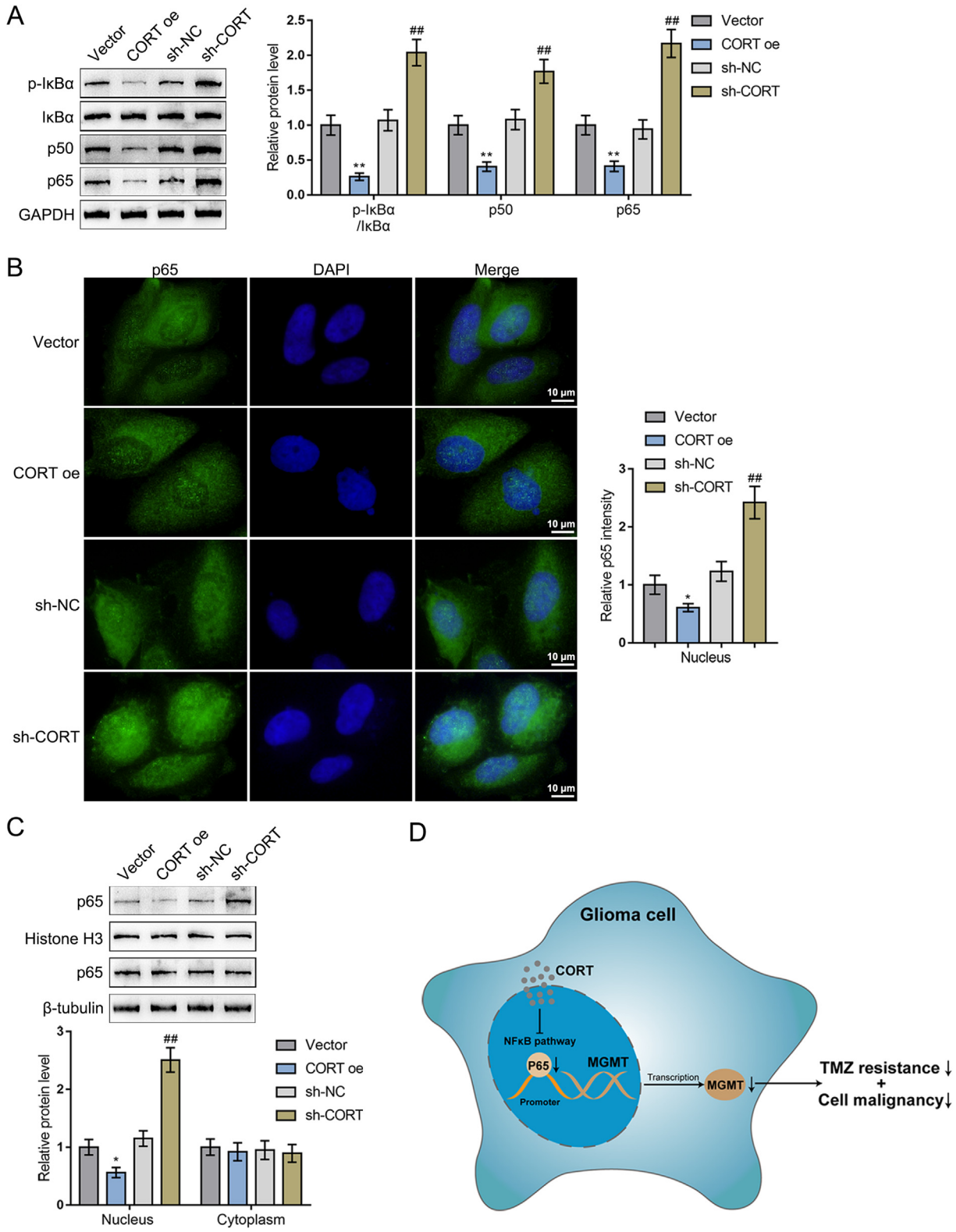

Figure 7 CORT inhibits the activation of the NF-κB pathway in glioma cells. **(A—C)** U251 cells were transfected with a CORT overexpression or knockdown vector and examined for the protein expression of p50 and p65 by Western blotting (A); the protein levels of p65 were determined by IF staining (B); and the protein levels of p65 in the cytoplasm and nucleus were separated and examined by Western blotting (C). **(D)** A schematic diagram of the proposed mechanism. The CORT/NF-κB/MGMT axis might be regarded as a molecular mechanism regulating the resistance of glioma to TMZ. Scale bar = 10 μm. $n = 3$; $^{*}P < 0.05$, $^{**}P < 0.01$, compared with the vector control group; $^{\#\#}P < 0.01$, compared with the sh-NC group.

Conclusion

Collectively, sufficient evidence was provided to reveal the specific effects of CORT on the TMZ resistance and progress of glioma. We found that CORT regulates glioma cell growth, migration, apoptosis, and TMZ resistance by weakening the activity of NF-κB/p65 in the regulation of MGMT expression. The CORT/NF-κB/MGMT axis might be regarded as the potential molecular regulatory mechanism of glioma resistance and prognosis to TMZ (Fig. 7D). These findings indicate that interfering with CORT expression in glioma may be considered a novel strategy for overcoming TMZ resistance in glioma treatment.

Ethics declaration

All procedures performed in studies involving human participants were in accordance with the ethical standards of Sichuan Provincial People's Hospital and the 1964 Declaration of Helsinki. Informed consent to participate in the study was obtained from all participants. Consent for publication was obtained from all participants.

Author contributions

Zongze He, Bo Peng, Qi Wang, and Jian Tang contributed to the experimental design and supervised the whole experimental process; Jie Tian, Ping Liu, and Jie Feng were involved in conducting the experiments; Yiwei Liao, Longyi Chen, and Ping Jia contributed to the data analysis and manuscript preparation. All authors read, revised, and approved the final manuscript.

Conflict of interests

The authors have no conflict of interests to report.

Funding

This study was supported by grants from the Department of Science and Technology of Sichuan Province, China (No. 23ZDYF2212, 23ZDYF2098), the Foundation for Sichuan Provincial People's Hospital (Sichuan, China) (No. 2022QN06), Medico-Engineering Cooperation Funds from the University of Electronic Science and Technology of China (No. ZYGX2021YGLH209) and 2022 Tianfu Qingcheng Project, China.

Data availability

Please contact the authors for data requests.

Acknowledgements

We thank the patients for their agreement to permit data collection and publication, and the staff at our institution for providing excellent patient care.

Appendix A. Supplementary data

Supplementary data to this article can be found online at https://doi.org/10.1016/j.gendis.2023.04.017.

References

1. Chen R, Smith-Cohn M, Cohen AL, Colman H. Glioma subclassifications and their clinical significance. *Neurotherapeutics*. 2017;14(2):284–297.
2. Gusyatiner O, Hegi ME. Glioma epigenetics: from subclassification to novel treatment options. *Semin Cancer Biol*. 2018;51:50–58.
3. Ostrom QT, Bauchet L, Davis FG, et al. The epidemiology of glioma in adults: a state of the science review. *Neuro Oncol*. 2014;16(7):896–913.
4. Bush NAO, Chang SM, Berger MS. Current and future strategies for treatment of glioma. *Neurosurg Rev*. 2017;40(1):1–14.
5. Xu S, Tang L, Li X, Fan F, Liu Z. Immunotherapy for glioma: current management and future application. *Cancer Lett*. 2020;476:1–12.
6. Choi S, Yu Y, Grimmer MR, Wahl M, Chang SM, Costello JF. Temozolomide-associated hypermutation in gliomas. *Neuro Oncol*. 2018;20(10):1300–1309.
7. Zhang J, Stevens MFG, Bradshaw TD. Temozolomide: mechanisms of action, repair and resistance. *Curr Mol Pharmacol*. 2012;5(1):102–114.
8. Tatar Z, Thivat E, Planchat E, et al. Temozolomide and unusual indications: review of literature. *Cancer Treat Rev*. 2013;39(2):125–135.
9. Lee SY. Temozolomide resistance in glioblastoma multiforme. *Genes Dis*. 2016;3(3):198–210.
10. Messaoudi K, Clavreul A, Lagarce F. Toward an effective strategy in glioblastoma treatment. Part I: resistance mechanisms and strategies to overcome resistance of glioblastoma to temozolomide. *Drug Discov Today*. 2015;20(7):899–905.
11. Ortiz R, Perazzoli G, Cabeza L, et al. Temozolomide: an updated overview of resistance mechanisms, nanotechnology advances and clinical applications. *Curr Neuropharmacol*. 2021;19(4):513–537.
12. Butler M, Pongor L, Su YT, et al. MGMT status as a clinical biomarker in glioblastoma. *Trends Cancer*. 2020;6(5):380–391.
13. Chen X, Zhang M, Gan H, et al. A novel enhancer regulates MGMT expression and promotes temozolomide resistance in glioblastoma. *Nat Commun*. 2018;9(1):2949.
14. Guo G, Sun Y, Hong R, et al. IKBKE enhances TMZ-chemoresistance through upregulation of MGMT expression in glioblastoma. *Clin Transl Oncol*. 2020;22(8):1252–1262.
15. Taniguchi K, Karin M. NF-κB, inflammation, immunity and cancer: coming of age. *Nat Rev Immunol*. 2018;18(5):309–324.
16. Tu J, Fang Y, Han D, et al. Activation of nuclear factor-κB in the angiogenesis of glioma: insights into the associated molecular mechanisms and targeted therapies. *Cell Prolif*. 2021;54(2),e12929.
17. Liu R, Chen Y, Liu G, et al. PI3K/AKT pathway as a key link modulates the multidrug resistance of cancers. *Cell Death Dis*. 2020;11(9):797.
18. Yu Z, Chen Y, Wang S, Li P, Zhou G, Yuan Y. Inhibition of NF-κB results in anti-glioma activity and reduces temozolomide-induced chemoresistance by down-regulating *MGMT* gene expression. *Cancer Lett*. 2018;428:77–89.
19. Gonzalez-Rey E, Pedreño M, Delgado-Maroto V, Souza-Moreira L, Delgado M. Lulling immunity, pain, and stress to sleep with cortistatin. *Ann N Y Acad Sci*. 2015;1351:89–98.

20. de Lecea L. Cortistatin: Functions in the central nervous system. *Mol Cell Endocrinol*. 2008;286(1—2):88—95.
21. Li M, Yan S, Fisher WE, Chen C, Yao Q. New roles of a neuropeptide cortistatin in the immune system and cancer. *World J Surg*. 2005;29(3):354—356.
22. Liang J, Bai Y, Chen W, Fu Y, Liu Y, Cortistatin Yin X. A novel cardiovascular protective peptide. *Cardiovasc Diagn Ther*. 2019;9(4):394—399.
23. Volante M, Rosas R, Allìa E, et al. Somatostatin, cortistatin and their receptors in tumours. *Mol Cell Endocrinol*. 2008; 286(1—2):219—229.
24. Cassoni P, Allia E, Marrocco T, et al. Ghrelin and cortistatin in lung cancer: expression of peptides and related receptors in human primary tumors and *in vitro* effect on the H345 small cell carcinoma cell line. *J Endocrinol Invest*. 2006;29(9): 781—790.
25. Notas G, Kolios G, Mastrodimou N, et al. Cortistatin production by HepG2 human hepatocellular carcinoma cell line and distribution of somatostatin receptors. *J Hepatol*. 2004;40(5): 792—798.
26. Ding C, Yi X, Chen X, et al. Warburg effect-promoted exosomal circ_0072083 releasing up-regulates NANGO expression through multiple pathways and enhances temozolomide resistance in glioma. *J Exp Clin Cancer Res*. 2021;40(1):164.
27. Cai T, Liu Y, Xiao J. Long noncoding RNA MALAT1 knockdown reverses chemoresistance to temozolomide via promoting microRNA-101 in glioblastoma. *Cancer Med*. 2018;7(4): 1404—1415.
28. Sun J, Ma Q, Li B, et al. RPN_2 is targeted by miR-181c and mediates glioma progression and temozolomide sensitivity via the Wnt/β-catenin signaling pathway. *Cell Death Dis*. 2020; 11(10):890.
29. De LL. Cortistatin: a natural somatostatin analog. *J Endocrinol Invest*. 2005;28(11 Suppl International):10—14.
30. Chiu CT, Wen LL, Pao HP, Wang JY. Cortistatin is induced in brain tissue and exerts neuroprotection in a rat model of bacterial meningoencephalitis. *J Infect Dis*. 2011;204(10): 1563—1572.
31. Wen Q, Ding Q, Wang J, et al. Cortistatin-14 exerts neuroprotective effect against microglial activation, blood-brain barrier disruption, and cognitive impairment in *Sepsis*-associated encephalopathy. *J Immunol Res*. 2022;2022, 3334145.
32. Oldrini B, Vaquero-Siguero N, Mu Q, et al. MGMT genomic rearrangements contribute to chemotherapy resistance in gliomas. *Nat Commun*. 2020;11(1):3883.
33. Wang X, Jia L, Jin X, et al. NF-κB inhibitor reverses temozolomide resistance in human glioma TR/U251 cells. *Oncol Lett*. 2015;9(6):2586—2590.
34. Happold C, Stojcheva N, Silginer M, et al. Transcriptional control of O6-methylguanine DNA methyltransferase expression and temozolomide resistance in glioblastoma. *J Neurochem*. 2018;144(6):780—790.
35. Li M, Liang RF, Wang X, Mao Q, Liu YH. BKM120 sensitizes C6 glioma cells to temozolomide via suppression of the PI3K/Akt/NF-κB/MGMT signaling pathway. *Oncol Lett*. 2017; 14(6):6597—6603.
36. Song T, Li H, Tian Z, Xu C, Liu J, Guo Y. Disruption of NF-κB signaling by fluoxetine attenuates MGMT expression in glioma cells. *OncoTargets Ther*. 2015;8:2199—2208.
37. Phillips RE, Soshnev AA, Allis CD. Epigenomic reprogramming as a driver of malignant glioma. *Cancer Cell*. 2020;38(5):647—660.
38. Allia E, Tarabra E, Volante M, et al. Expression of cortistatin and MrgX2, a specific cortistatin receptor, in human neuroendocrine tissues and related tumours. *J Pathol*. 2005;207(3): 336—345.
39. Cassoni P, Muccioli G, Marrocco T, et al. Cortistatin-14 inhibits cell proliferation of human thyroid carcinoma cell lines of both follicular and parafollicular origin. *J Endocrinol Invest*. 2002; 25(4):362—368.
40. Luque RM, Villa-Osaba A, L-López F, et al. Lack of cortistatin or somatostatin differentially influences DMBA-induced mammary gland tumorigenesis in mice in an obesity-dependent mode. *Breast Cancer Res*. 2016;18(1):29.
41. McDuff SGR, Dietrich J, Atkins KM, Oh KS, Loeffler JS, Shih HA. Radiation and chemotherapy for high-risk lower grade gliomas: choosing between temozolomide and PCV. *Cancer Med*. 2020; 9(1):3—11.
42. Hombach-Klonisch S, Mehrpour M, Shojaei S, et al. Glioblastoma and chemoresistance to alkylating agents: involvement of apoptosis, autophagy, and unfolded protein response. *Pharmacol Ther*. 2018;184:13—41.
43. Yi GZ, Huang G, Guo M, et al. Acquired temozolomide resistance in MGMT-deficient glioblastoma cells is associated with regulation of DNA repair by DHC2. *Brain*. 2019;142(8): 2352—2366.
44. DiDonato JA, Mercurio F, Karin M. NF-κB and the link between inflammation and cancer. *Immunol Rev*. 2012;246(1):379—400.
45. Hoesel B, Schmid JA. The complexity of NF-κB signaling in inflammation and cancer. *Mol Cancer*. 2013;12:86.
46. Duan S, Li M, Wang Z, Wang L, Liu Y. H19 induced by oxidative stress confers temozolomide resistance in human glioma cells via activating NF-κB signaling. *OncoTargets Ther*. 2018;11: 6395—6404.
47. Wu K, Bonavida B. The activated NF-kappaB-Snail-RKIP circuitry in cancer regulates both the metastatic cascade and resistance to apoptosis by cytotoxic drugs. *Crit Rev Immunol*. 2009;29(3):241—254.
48. Hu YH, Jiao BH, Wang CY, Wu JL. Regulation of temozolomide resistance in glioma cells via the RIP2/NF-κB/MGMT pathway. *CNS Neurosci Ther*. 2021;27(5):552—563.